First publ. in: Biophysical Journal 76 (1999), 1, pp. 509-516

Imaging of Cell/Substrate Contacts of Living Cells with Surface Plasmon Resonance Microscopy

K.-F. Giebel,* C. Bechinger,* S. Herminghaus,* M. Riedel,*P. Leiderer,* U. Weiland,# and M. Bastmeyer#
*Faculty for Physics and #Faculty for Biology, University of Konstanz, D-78457 Konstanz, Germany

ABSTRACT We have developed a new method for observing cell/substrate contacts of living cells in culture based on the optical excitation of surface plasmons. Surface plasmons are quanta of an electromagnetic wave that travel along the interface between a metal and a dielectric layer. The evanescent field associated with this excitation decays exponentially perpendicular to the interface, on the order of some hundreds of nanometers. Cells were cultured on an aluminum-coated glass prism and illuminated from below with a laser beam. Because the cells interfere with the evanescent field, the intensity of the reflected light, which is projected onto a camera chip, correlates with the cell/substrate distance. Contacts between the cell membrane and the substrate can thus be visualized at high contrast with a vertical resolution in the nanometer range. The lateral resolution along the propagation direction of surface plasmons is given by their lateral momentum, whereas perpendicular to it, the resolution is determined by the optical diffraction limit. For quantitative analysis of cell/substrate distances, cells were imaged at various angles of incidence to obtain locally resolved resonance curves. By comparing our experimental data with theoretical surface plasmon curves we obtained a cell/substrate distance of 160 $\pm$ 10 nm for most parts of the cells. Peripheral lamellipodia, in contrast, formed contacts with a cell substrate/distance of 25 $\pm$ 10 nm.

INTRODUCTION

Movement of cells on planar substrates is characterized by the temporary formation of cell/substrate contacts. The cell membrane is usually separated from the substrate by 100–150 nm. In the case of cell/substrate adhesion two different types of contacts have been described: focal contacts, in which small regions of the cell (1 μm width and 2–10 μm length) reach the substrate by 10–15 nm, and close contacts, in which broad areas of the lamellipodium are separated from the substrate by 30 nm (Izzard and Lochner, 1976).

These cell/substrate contact sites in living cells in culture are usually studied with interference reflection microscopy (IRM) or with total internal reflection fluorescence microscopy (TIRFM). With the IRM method the cell is illuminated by visible light through a transparent glass support and the light is partially reflected from different interfaces on its way through the semitransparent sample (Curtis, 1964). The image results from an interference pattern of the reflected light beams. This technique allows visualization of cell/substrate contacts at high contrast, but quantitative measurements of membrane/substrate distances must be interpreted with caution (Verschueren, 1985). For the TIRFM method, the cell membrane is labeled with a fluorescent dye. The dye is then excited by an evanescent wave of a totally reflected light beam that preferentially illuminates regions of the membrane nearest the substrate (Axelrod et al., 1983). Here, quantitative measurements of cell/substrate contacts can be obtained when the cells are analyzed under variable angle excitation (Burmeister et al., 1994, 1998). Recently, a new fluorescence technique, fluorescence interference-contrast (FLIC) microscopy, has been introduced to measure cell/substrate distances of cells growing on a nontransparent substrate. Here, a standing light wave in front of the reflecting surface of a silicone support was used to modulate the excitation and emission of fluorescent dyes incorporated into the cell membrane (Braun and Fromherz, 1997).

In this paper we describe a technique for visualizing and quantifying cell/substrate contacts based on the optical excitation of surface plasmons. Surface plasmons are generally referred to as quanta of an electromagnetic wave that travels along the interface between a metal and a dielectric layer. Due to boundary conditions, the electric field associated with this excitation decays perpendicular to the surface. In contrast to IRM, this decay is exponential and typically on the order of some hundreds of nanometers. The resulting concentration of the electromagnetic field close to the surface makes surface plasmons sensitive to even minute changes in interface processes (Raether, 1988). The vertical resolution is theoretically in the sub-nanometer range and, therefore, at least one order of magnitude higher than that of IRM. In the biosciences, surface plasmons are usually used in optical biosensors to monitor molecular interactions such as receptor/ligand binding in real time (Panayotou et al., 1993). We have built a surface plasmon microscope (SPM), originally described by Rothenhäusler and Knoll (1988), to analyze the contacts of cells growing on an aluminum-coated glass support. With this new technique we were able to visualize cell/substrate contacts at high contrast and to quantify membrane/substrate distances in the nm range.

Received for publication 18 February 1998 and in final form 23 September 1998.

Address reprint requests to Dr. Martin Bastmeyer, University of Konstanz Faculty for Biology, M626, D-78457 Konstanz, Germany. Tel.: 07531-88-2624; Fax: 07531-88-3894; E-mail: martin.bastmeyer@uni-konstanz.de.

MATERIALS AND METHODS

Description of the microscope

For the interpretation of our results, it was necessary to observe cells in the surface plasmon microscope (SPM) and in an optical microscope at the same time. Therefore, a miniaturized SPM was built that could be directly

attached to an upright microscope (Axioplan, Zeiss, Jena, Germany). The setup is shown schematically in Fig. 1. The SPM consists essentially of two arms carrying the optical components for illuminating and imaging the base of a glass prism. The prism is coated with a 15-nm layer of aluminum (Al) to allow optical excitation of surface plasmons. The angle between the two arms can be adjusted to obtain the condition for the occurrence of plasmon resonance. The beam diameter of a laser diode (LD) (3 mW, λ = 670 nm) is increased to about 5 mm by means of a beam expander (BE) and then strikes a mirror (M) mounted on a motor-controlled rotation stage. The reflected laser beam is then guided to the Al-coated base of the glass prism by two positive lenses, L1 and L2, which guarantee that the beam always illuminates the same area of the prism base regardless of the mirror position. Because surface plasmons are excited only with p-polarized light, a linear polarizer (P) is placed between L1 and L2. The reflected light is imaged with a microscope objective (L3) (Achromat LDN, 20x/0.35, Carl Zeiss, Jena, Germany) and an eyepiece (L4) (Zeiss, 12, 5x) onto a camera chip (CCD, Hamamatsu, Herrsching, Germany) and stored on a computer. The SPM is attached to the stage of an upright microscope equipped with epi-illumination optics and a long-distance water-immersion lens (Achroplan 20x/0.5w, Zeiss). The image is focused onto a second CCD camera, which is also connected to an imaging processing system.

Cell culture

Cell adhesion phenomena were studied using primary goldfish glial cell cultures. The main advantage of these cells over mammalian cell lines is that they can be cultured at room temperature in Hepes-buffered medium. The isolation of goldfish glial cells and culture conditions have been described in detail (Bastmeyer et al., 1993, 1994). In brief, small pieces from regenerating optic nerves and tracts from adult goldfish 2 weeks after optic nerve section were incubated at 28°C for 20 min in Leibovitz medium (L15) with 0.3% collagenase (Worthington Seromed, Berlin, Germany) and 0.1% dispase (Boehringer Mannheim, Mannheim, Germany). The enzyme mixture was replaced by L15 with 20% fetal calf serum and centrifuged at 200 $\times$ *g* for 5 min. The tissue was then resuspended in F12 culture medium (Ham's F-12, Gibco-BRL (Gaithersburg, MD), supplemented with 10% fetal calf serum, 0.4% methylcellulose, 50 mM Hepes, and 80 μM penicillin/streptomycin) and plated onto polylysine/laminin-coated coverslips. These primary cultures were grown at 27°C to high density. They contain mainly oligodendrocytes which associate into a network-like carpet, astrocytes which form separate clusters, and some fibroblasts (Bastmeyer et al., 1993, 1994). After 3–4 weeks, glial cells were removed from the coverslip with a rubber spatula, immersed in F12 culture medium, and re-explanted onto an aluminum-coated glass prism (for surface plasmon resonance microscopy, or SPRM), an aluminum-coated coverslip (for atomic force microscopy, or AFM), or a polylysine-coated coverslip (for IRM).

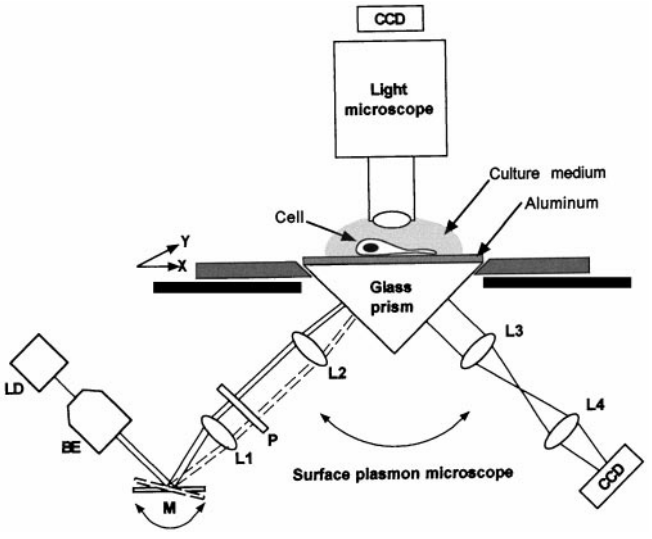

FIGURE 1 Schematic drawing of a surface plasmon microscope. Cells were cultured on an aluminum-coated glass prism and observed from above with a conventional light microscope. The lower surface of the cells is simultaneously investigated with surface plasmon microscopy. For further explanations, see Materials and Methods. Abbreviations: BE, beam expander; CCD, camera chip; LD, laser diode; L1-L4, lenses; M, mirror; P, polarizer.

IRM of living cells

For IRM, glass coverslips with adhering glial cells were removed from the culture dish, wiped dry on the bottom surface, inverted, and placed on a glass slide. Small glass spacers were placed between the slide and the coverslip. The region between the two glasses was filled with culture medium. Cells were observed on an upright microscope (Axioplan, Zeiss) with phase contrast and IRM optics using a 63x/1.25 oil antiflex objective (Zeiss). Pictures were taken with a video camera (Newicon, Hamamatsu) and stored on a computer.

AFM of fixed cells

To prevent height artifacts due to the loading force of the AFM tip, oligodendrocytes were fixed in 1% glutaraldehyde in phosphate-buffered saline for 5 min. No swelling or shrinkage due to fixation was observed under these conditions; the cells were mechanically stable and could be scanned with the AFM tip without damage. Scanning force microscopy was carried out in liquid phosphate-buffered saline with a Topometrix Discoverer TMX 2010 equipped with silicon nitride probes (single beam cantilevers 200 $\times$ 20 μm with oxide-sharpened pyramidal tips, Olympus, Tokyo, Japan).

RESULTS AND DISCUSSION

Description and principles of the method

There is a vast amount of literature on how to optically excite surface plasmons (Knoll, 1991; Sambles et al., 1991). Therefore, we discuss the technique only briefly here.

Let us consider a boundary (*x*,*y*-plane) between two dielectric materials with dielectric constants $\epsilon_1 = \epsilon_1' + i\,\epsilon_1''$ and $\epsilon_2 = \epsilon_2' + i\,\epsilon_2''$, respectively. For an electromagnetic surface wave of frequency ω propagating along the boundary in *x* direction, we expect the following behavior:

$$\vec{E} = \vec{E}_0 e^{-i(k_x x + k_{z,l} z - \omega t)}, \quad l = 1, 2 \tag{1}$$

where k_z is imaginary. Accordingly, the amplitude of the electromagnetic field associated with the surface plasmons has its maximum right at the boundary and decays exponentially perpendicular to the surface. From Maxwell's equations one then obtains the dispersion relations along the *x* and *z* directions:

$$k_x^2 = \frac{\omega^2}{c^2}\left(\frac{\epsilon_1 \epsilon_2}{\epsilon_1 + \epsilon_2}\right) \tag{2}$$

and

$$k_{z,l}^2 = \frac{\omega^2}{c^2}\left(\frac{\epsilon_l^2}{\epsilon_1 + \epsilon_2}\right) \tag{3}$$

We will consider only dielectrics with no dielectric losses, i.e., $\epsilon'' = 0$. Then Eqs. 2 and 3 can both be fulfilled only for $\epsilon_1 + \epsilon_2 < 0$. This corresponds to a metal-dielectric surface. Assuming the dielectric constant of the metal being described by the Drude model,

$$\epsilon_1(\omega) = 1 - \omega_P^2/\omega^2 \tag{4}$$

with ω_P being the plasma frequency of the metal, one obtains the dispersion relation of the surface plasmons by inserting Eq. 4 in Eq. 2:

$$\kappa_x^2 = \frac{\omega^2}{c^2}\frac{\epsilon_2(1 - \omega_P^2/\omega^2)}{(\epsilon_2 + 1 - \omega_P^2/\omega^2)} \tag{5}$$

For real metals we expect the dispersion relation to be slightly different due to electronic losses. Eq. 5, however, is a good approximation for the visible spectrum.

In the following we will describe how surface plasmons can be excited by optical means using the so-called Kretschmann setup, in which the metal film is deposited on top of a glass prism with dielectric constant ϵ_g. This metal film is illuminated with a p-polarized, parallel beam from inside the prism under total internal reflection conditions, as shown in Fig. 2 *A*. When the angle of incidence Θ, which determines the in-plane wave number of the incoming light $K_x = \sqrt{\epsilon_g}\,\omega/c \sin\Theta$, matches the propagation constant of surface plasmons at the metal/air interface, i.e., $K_x = k_x$, this mode is resonantly excited at the expense of the reflected light. This leads to a pronounced dip in reflectivity at the resonance angle Θ_1 (Fig. 2 *C*, *solid line*). The reflectivity curve can be calculated by the method of transfer matrices, which is often employed for light propagation in layered systems (Macleod, 1986).

As already mentioned, the electric field (evanescent wave) associated with surface plasmons decays exponentially with a characteristic decay length κ perpendicular to the interface and is therefore confined to a narrow region at the metal surface (Fig. 2 *A, shaded area*). When a dielectric material is brought into the region of the evanescent field (Fig. 2 *B*) it modifies the propagation constant of the surface plasmons, resulting in a shift of the angle of resonance (Fig. 2 *C, dashed curve*). If the dielectric constant of the material is known, the distance to the metal can be calculated from this shift (Knoll, 1991). This feature makes surface plasmons a very sensitive probe for studying processes in the vicinity of metal surfaces.

Next, we applied this technique to cultured cells as the dielectric on top of a metal layer. As mentioned in the Introduction, the cell/substrate distance is expected to vary locally across the surface. Accordingly, the angle of resonance will also vary for different sites and therefore the reflectivity (*R*) of those sites will be different for a fixed angle of incidence (Fig. 2 *D*). Imaging the reflected light onto a CCD camera chip then yields a high-contrast image of the spatial distribution of cell/substrate distances across the sample. Quantitative information about distances can be achieved if the sample is illuminated under different angles

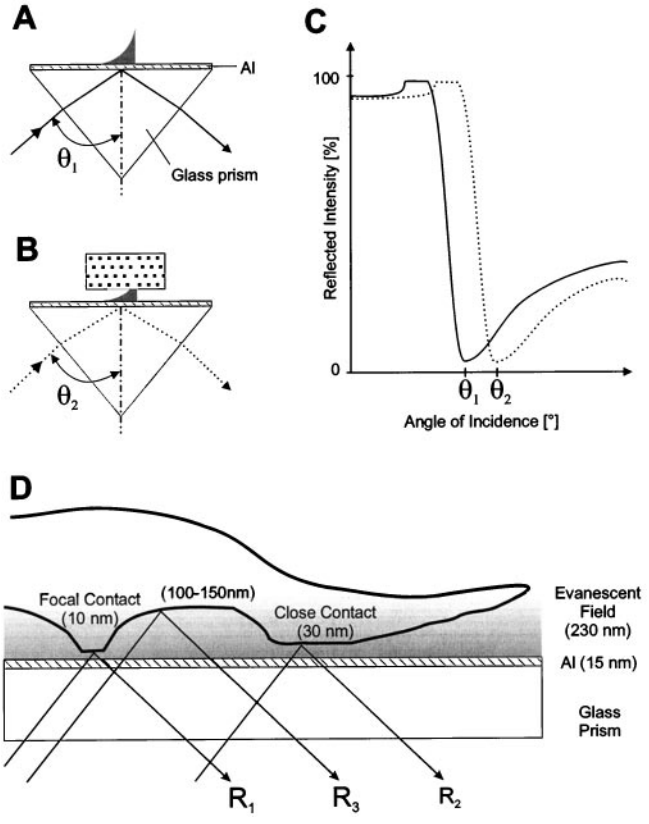

FIGURE 2 Principle of surface plasmon microscopy. (*A*) Excitations of surface plasmons on a metal/air interface at the base of an aluminum-coated (Al) glass prism by total reflection of a laser beam at a resonance angle θ_1. An evanescent field is created (*shaded area*) that decays perpendicular to the surface. (*B*) When a dielectric body (*dotted area*) is brought into the region of the evanescent field, resonant excitation of surface plasmons is shifted to larger angles $\theta_2 > \theta_1$. (*C*) Corresponding reflectivity curves of *A* (*solid line*) and *B* (*dotted line*). (*D*) Schematic drawing of a lamellipodium of a cell inside the evanescent field. Depending on the local cell/substrate distance, a characteristic reflected intensity R_i is obtained. This intensity varies greatly for focal contacts, close contacts, and other areas of the cell membrane.

of incidence, which is achieved in our setup by rotating the mirror (M in Fig. 1). From the sequence of pictures obtained, we can calculate resonance curves (as in Fig. 2 *C*) for individual sites of the sample. The local cell/substrate distances can then be determined from those curves.

Lateral resolution

In addition to a sensitive contrast mechanism, microscopic techniques also need lateral resolution to enable observers to distinguish structures on a sample. In conventional microscopy, the lateral resolution is limited by diffraction of the illuminating light. This, however, does not generally apply for SPRM. During optical excitation, surface plasmons pick up horizontal momentum from the incident photons. Therefore, they propagate along the metal/dielectric interface until they finally decay back into photons or dissipate into heat (Knoll, 1991). Consequently, surface plas-

mons cannot resolve features below their propagation length Λ parallel to the incident plane, whereas diffraction-limited resolution is obtained perpendicular to it. For a 53-nm-thick silver (Ag) film, Λ is calculated to be about 40 μm at a wavelength of 633 nm (Raether, 1988). This is demonstrated in the test pattern shown in Fig. 3, *A* and *B*. The structure consists of a 53-nm thick homogenous Ag film and a 20-nm Ag layer evaporated through a grid with quadratic openings of 6×6 μm and a periodicity of 12 μm. Fig. 3 *A* is an interference reflection picture of the pattern, whereas Fig. 3 *B* is an image of the same pattern obtained by SPRM. As is clearly visible in the SPRM image, the quadratic features are smeared out to a bright band along the direction of SP propagation (horizontal), whereas perpendicular to it the structure is resolved. Fig. 3, *C* and *D*, shows the corresponding results for the same pattern made of 15-nm (+7-nm) Al. In contrast to Ag, the test pattern is now clearly resolved even in the propagation direction and an image analysis leads to a lateral resolution below 1 μm, which is sufficient for many biological systems. The higher resolution in the case of Al is due to its larger absorptivity at the illuminating wavelength, which decreases the propagation length of the surface plasmons. This is also evident from the corresponding resonance curves in Fig. 3 *E*. In the case of Ag (*dashed line*) the resonance width is below one degree, whereas in the case of Al (*solid line*) the halfwidth of the resonance, being inversely proportional to Λ, is much higher. However, because the slope of the resonance is steeper for Ag than for Al, the advantage of having a smaller Λ is somewhat compensated by a smaller sensitivity of the surface plasmons to material contrast.

Besides having the better lateral resolution, Al is also more compatible with biological systems. We assume this is due to the native oxide layer that is known to form on Al films. This layer is chemically inert and very stable and provides a good substrate for biological systems.

Microscopy of living cells

When goldfish oligodendrocytes are grown on polylysine-coated glass coverslips they are highly motile and move considerable distances over the substrate (Bastmeyer et al., 1994). Phase-contrast images show that the oligodendrocytes typically form a leading and a trailing lamellipodium. Both lamellipodia consist of an organelle-rich central region (Fig. 4 *A*, *asterisks*) and a peripheral region which contains few organelles (Fig. 4 *A*, *arrowheads*). IRM reveals that the area between the two lamellipodia is uniformly light gray, indicating a distance between the cell membrane and the substrate of more than 100 nm. The organelle-sparse regions of the leading and trailing lamellipodia, however, appear black (Fig. 4 *B*), indicating a close contact (below 30 nm) between the membrane and the substratum in these regions. No focal contacts, defined as very dark streaks (Verschueren, 1985), can be observed in goldfish oligodendrocytes. Thus, IRM shows that goldfish oligodendrocytes form cell/substrate contacts that are typical of other highly motile cells (Kolega et al., 1982).

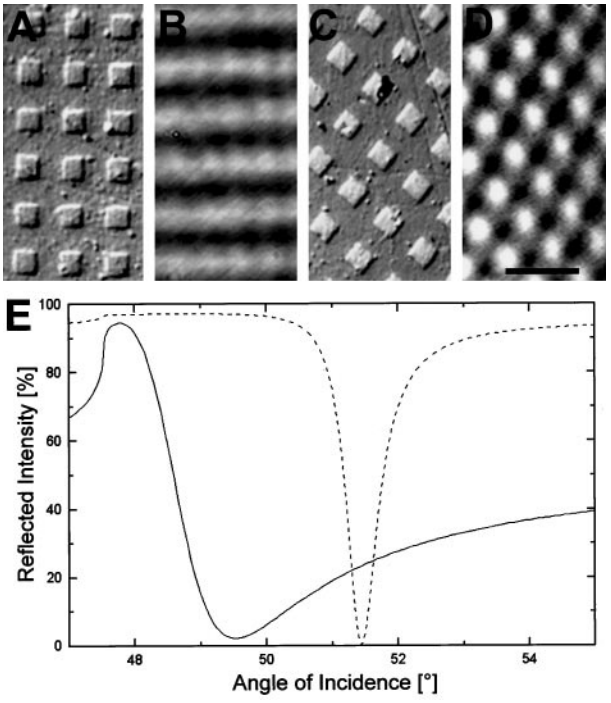

FIGURE 3 Lateral resolution of the surface plasmon microscope. Optical microscope images of a silver (*A*) and aluminum (*C*) test structure. Corresponding SPM images (*B*, *D*) of the test patterns with the direction of illumination being from left to right. In the case of silver, the square shaped structures (6×6 μm) are not resolved horizontally due to the propagation of surface plasmons, whereas SPRM on aluminum provides a resolution of about 1 μm. (*E*) Calculated surface plasmon resonance curves for silver (*dotted line*) and aluminum (*solid line*). Scale bar in $D = 20$ μm.

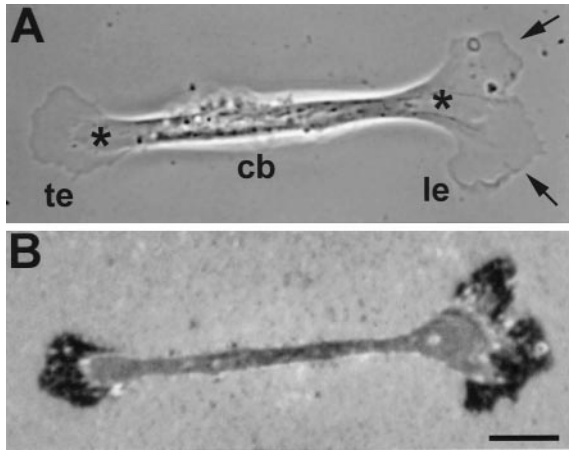

FIGURE 4 Interference reflection microscopy of a goldfish glial cell. Bipolar goldfish oligodendrocyte in phase contrast (*A*) and interference reflection contrast (*B*). Arrows in *A* point to the thin peripheral lamellipodium. Organelle-rich regions of the leading edge (le) and trailing end (te) are marked by asterisks. In the IRM image only the peripheral parts of both lamellipodia show low reflectivity and appear black, indicating close contact with the substrate. Other parts of the cell including the cell body (cb) appear uniformly gray. Scale bar = 50 μm.

Next, we observed goldfish oligodendrocytes with surface plasmon microscopy. Cells were plated onto an aluminum-coated glass prism, where they adhered to the substrate, formed lamellipodia, and began to migrate after 3–4 h. The oligodendrocytes were also observed from above with an optical microscope and a water-immersion lens under epi-illumination conditions. Because the cells grow on a metal film, the reflected light reveals the cell morphology (Fig. 5 *A*). Simultaneously, the same cells were visualized with SPRM. As explained above, the contrast in SPRM can be varied and depends on the incident angle. We adjusted the incident angle so that the aluminum substrate was in resonance and appeared uniformly dark gray. Under these settings the leading and trailing lamellipodia were visible with SPRM, indicating that these parts of the cell are in close contact (below 230 nm) to the substrate (Fig. 5 *B*). Furthermore, the reflected intensity correlates with the cell/substrate distance: the closer the membrane is to the substrate, the more light is reflected. When the cells migrated over the aluminum substrate, cell/substrate contacts were broken and newly formed, leading to local changes in the reflected intensity. This becomes most obvious in Fig. 5 *C*, which shows an image obtained by subtraction of two SPM images with a time interval of 2 min. In this difference image, only those areas where the cell/substrate distance has changed during the time interval are visible. White areas indicate where the cell membrane has approached the substrate, whereas black means that the cell membrane has moved further away from the substrate.

Thus, SPRM provides a valuable tool for visualizing cell/substrate contacts of living cells at high contrast.

Quantitative measurements

In addition to qualitative information, SPRM also provides quantitative data regarding the cell-substrate distances. To demonstrate this, we imaged ten glial cells in the SPM at various angles of incidence and stored the pictures on a computer. An example is shown in Fig. 6. As can be seen, even a small change in the angle of incidence (θ) causes a strong change in the intensity contrast (Fig. 6 *C*) that is typical for a plasmon resonance. From the analysis of 200 pictures taken at different angles, we obtained locally resolved resonance curves. In Fig. 6, *D*, *E*, and *F*, the results at three different characteristic sites are shown as symbols. The sites are indicated in Fig. 6 *A* and correspond to locations where different cell/substrate distances are expected: (1) no cell, (2) central lamellipodium, and (3–4) peripheral lamellipodium. The solid and dashed lines are fits to the data and are discussed below.

All experimental curves show essentially the same shape. With increasing angle of incidence Θ, the reflectivity increases until the critical angle of total reflection is reached. For larger Θ, an asymmetrical resonance appears that is characteristic for a surface plasmon resonance on Al, as can be seen by comparison with Fig. 3 *E*.

Next, we compare our experimental data with theoretical surface plasmon curves. Our calculations are based on a multilayer system on top of a glass prism consisting of (i) an Al film of $d_{Al} = 15$ nm thickness, (ii) media of thickness d_M, (iii) the cell of thickness d_C, and (iv) a layer of media above the cell. Because the last layer can be assumed to be large compared to the decay length of the evanescent field κ, it need not be considered as a fit parameter. In all of the following calculations, cell membranes with a thickness of $d_{Me} = 4$ nm were taken into account, even if not mentioned explicitly. The corresponding refractive indices of media, cell, and membrane were taken from the literature (Izzard and Lochner, 1976), i.e., $n_M = 1.336$, $n_C = 1.356$, and $n_{Me} = 1.46$, respectively.

First, we fitted the experimental curve shown in Fig. 6 *D*, which is typically found at regions of the prism without

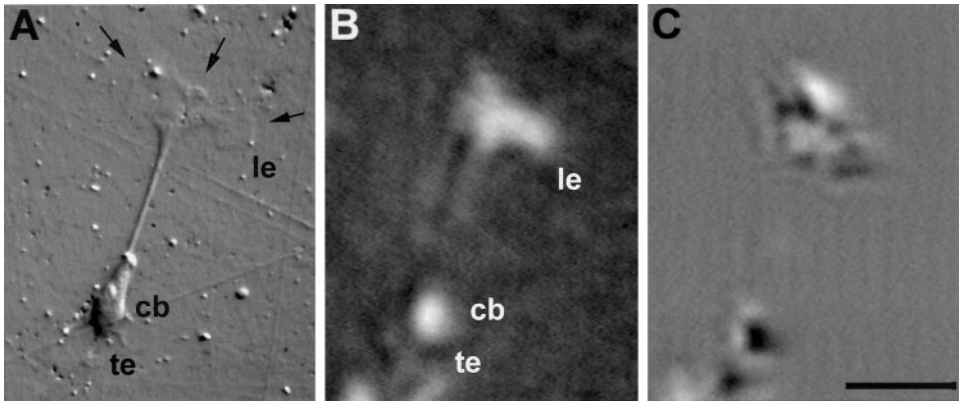

FIGURE 5 Surface plasmon microscopy of a goldfish glial cell. Living goldfish oligodendrocyte on an aluminum substrate in epi-illumination (*A*) and SPRM (*B*). This bipolar cell moved toward the upper right during imaging. The arrows in *A* point to the lamellopodium of the leading edge (le). In the SPRM image (*B*), lamellopodia of the leading edge (le) and the trailing end (te) and parts of the cell body (cb) are visible, indicating a that these areas have a cell/substrate distance < 230 nm. The difference image (*C*) illustrates changes in cell/substrate distances that occurred within 2 min after (*B*) was taken. Here, black indicates that the cell membrane has moved away from the substrate, whereas white indicates newly formed cell/substrate contacts. In the SPRM images the direction of illumination is from left to right. Scale bar = 100 μm

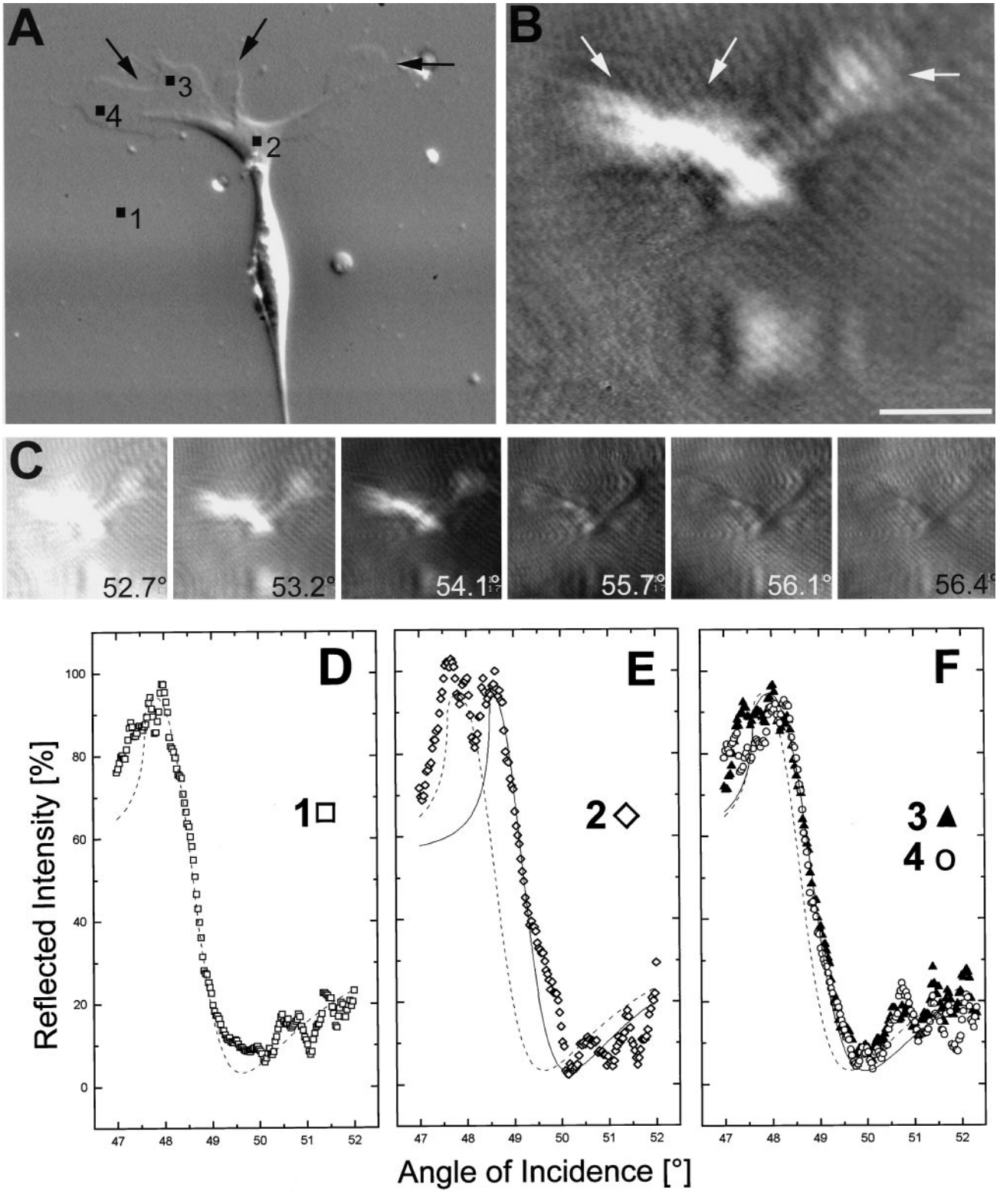

FIGURE 6 Quantification of cell/substrate distances. Interference contrast (*A*) and corresponding SPRM image (*B*) of a goldfish glial cell on an aluminum substrate. Corresponding parts of the leading edge are marked with arrows in *A* and *B*. *C*: The same cell with different angles of illumination. Depending on the angle of incidence different sites of the cell are in resonance and therefore the contrast of the SPRM picture changes. *D-F*: Reflectivity curves for locations 1–4 (marked in *A*): *D*, bare substrate (□); *E*, thick, organelle-rich part of the lamellipodium (◇); *F*, thin part of the lamellipodium (▲ and ○). The dashed line in *D* is a fit to the undisturbed surface plasmon curve of the bare substrate and is replotted in *E* and *F* as a reference. The solid lines in *E* and *F* are the calculated plasmon curves for regions of the central (*E*) and peripheral lamellipodium (*F*). Scale bar in (*B*) = 100 μm.

adhering cells. The calculations are based on a two-layer system consisting of an Al film 15 nm thick and an infinite layer of culture medium. From the fit (*dashed line*), we determined the refractive index and the extinction coefficient α_{Al} of the Al film to be $n_{Al} = 1.2116$ and $\alpha_{Al} = 6.7736$, respectively. Both values are very close to the corresponding values found in the literature (Driscoll and Vaughan, 1978). Next, we analyzed the data shown in Fig. 6 *E*. Corresponding to a site below the central lamellipodium, the reflectivity is shifted to larger angles, as can be seen by the dashed line replotted from Fig. 6 *D*. Here, we assumed d_C to be large compared to the decay length of the evanescent field ($\kappa = 230$ nm). This assumption is justified by our own AFM measurements, which yielded values of d_C well above 400 nm. Accordingly, the situation can be described by an Al/medium/cytoplasm layer system with a single fitting parameter, namely the cell/substrate distance, d_M. The solid line in Fig. 6 *F* is a least mean squares fit with $d_M = 160 \pm 10$ nm. This value for the cell/substrate distance is in excellent agreement with results of other authors (Izzard and Lochner, 1976; Verschueren, 1985). Cell/substrate distances can thus be quantified easily with SPRM in regions where the cell's thickness surpasses the penetration depth of surface plasmons, in our case 230 nm.

To determine the cell/substrate distance at the peripheral lamellipodium (Fig. 6 *E*), one has to know the thickness of the cell (d_C) in this region; otherwise, an unambiguous solution of d_M (i.e., the cell/substrate distance) is not possible. This additional information is essential not only to our technique, but also to all other experiments in which cell/substrate distances are measured by optical means, as discussed in detail below. We measured the thickness of the lamellipodium of slightly fixed oligodendrocytes adhering to Al-coated coverslips with atomic force microscopy (Fig. 7). The heights of peripheral lamellipodia were determined and averaged over squares of 4 μm^2. In 14 AFM scans of 8 different lamellipodia, we obtained a mean height of 60 nm $\pm$ 20 nm. In contrast, the organelle-rich central region of the lamellipodium has a height of several hundred nm, whereas the cell body is in the range of several μm. It is not clear whether the 60-nm value obtained with AFM represents the total thickness of the lamellipodium (i.e., the lamellipodium is pushed to the surface by the AFM tip) or the thickness of the lamellipodium plus the membrane/substrate distance. Therefore, the data in the region of the lamellipodium are modeled for the two extreme cases with the following layer system: Al/medium/cytoplasma/medium, with the second medium layer again assumed to be large compared to κ. First, we assumed a thickness of the lamellipodium $d_C = 60$ nm in this region, and only the cell/substrate distance d_M as fitting parameter was left. The best agreement with the data in Fig. 6 *E* is obtained with $d_M = 30 \pm 10$ nm (*solid line*). Second, we assumed a thickness of the lamellipodium plus the cell/substrate distance of 60 nm. In this case we obtained a cell/substrate distance $d_M = 18$ nm, leaving 42 nm for the thickness of the lamellipodium. Therefore, we can determine the cell/substrate distance at peripheral lamellipodia to be within the range of 25 $\pm$ 10 nm.

Comparison of SPRM and other methods

The values we obtained with SPRM (25 $\pm$ 10 nm for close contacts and 160 $\pm$ 10 nm for other parts of the cell) are in good agreement with those obtained by other methods. Using IRM, Izzard and Lochner (1976) reported a cell/substrate distance of 30 nm for close contacts and 100–140 nm for other regions of fibroblasts. In principle, IRM has a lateral resolution of 0.2 μm and 1 nm in the vertical plane (Rädler and Sackmann, 1993). However, it is now widely accepted that quantitative measurements of cell/substrate distances with IRM are only possible with a cytoplasmic layer at least 1 μm thick (Verschueren, 1985). In thin lamellipodia, for example, reflections from the upper surface of the cell interfere with reflections from the lower surface and can completely invalidate conclusions about cell/substrate distances (Gingell, 1981). In these regions,

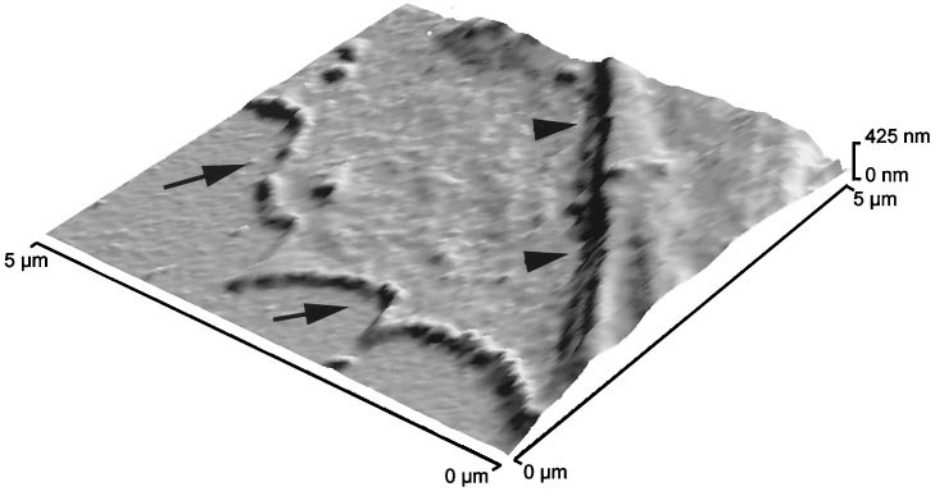

FIGURE 7 Atomic force microscopy image of the lamellipodium of a fixed goldfish oligodendrocyte. The thin, peripheral region of the lamellopodium (*arrows*) has a mean height of 60 nm, whereas in the organelle-rich region (*arrowheads*) the height increases to several hundreds of nanometers.

even a qualitative interpretation of the image is hazardous (Verschueren, 1985). This problem can be overcome when the principles of IRM optics are combined with the vertical resolution of a laser scanning microscope (Paddock, 1989). Using this method of tandem scanning confocal microscopy, Davies et al. (1993, 1994) have analyzed cell-substratum adhesion in endothelial cells. They report a cell/substrate distance of 10–15 nm for focal contacts and 30–100 nm for close contacts (Davies et al., 1993).

An alternative method for investigating cell/substrate contacts is TIRFM (Axelrod et al., 1983), in which a fluorescent dye is used to label the cell membrane and then excited by an evanescent wave. Quantitative measurements of cell/substrate distances can be obtained with this method when the same cell is examined with multiple angles of the illumination beam, as was reviewed by Burmeister et al. (1994, 1998). Lanni and co-workers were the first to apply TIRFM to quantify cell/substrate distances of fibroblasts; they estimated a separation distance of 69 nm for close contacts and 49 nm for focal contacts (Lanni et al., 1985). Recently, a new method also involving fluorescent labeling of the cell membrane, FLIC microscopy, has been established. In FLIC microscopy the dye is illuminated and excited by standing modes of light in front of a reflecting silicon surface (Braun and Fromherz, 1997). The cell/substrate distances of membranes of red blood cell ghosts were found to be 12 nm. Measurements of cell/substrate distances of living cells have not yet been made with this method. Both methods involving the excitation of a fluorescent dye incorporated into the cell membrane, FLIC microscopy and TIRFM, are valuable tools for visualizing and measuring cell/substrate distances, but in thin areas of the cell quantitative analysis is hampered by fluorescence from the upper membrane. Therefore, both methods require additional information about the cell's thickness in areas of peripheral lamellipodia to determine cell/substrate distances unambiguously. This additional information, however, is essential for all the methods discussed here (IRM, FLIC microscopy, and TRIFM), because an optical experiment cannot distinguish between the different interfaces.

In summary, our findings show that SPRM can be used as an alternative and additional method for visualizing and quantifying cell/substrate contacts of living cells. A disadvantage of SPRM is reduced lateral resolution due to the propagation of surface plasmons parallel to the incident plane. However, in contrast to IRM, SPRM works on semitransparent metal surfaces. These metal-coated surfaces are required to produce self-assembled monolayers, a technique that in combination with microcontact printing allows the adsorption of proteins in a well-ordered form onto surfaces (Mrksich and Whitesides, 1996). Therefore, SPRM offers a new, powerful tool to study cell adhesion phenomena on these micropatterned substrates.

We thank Ulrike Binkle for technical assistance with cell culture work and Mary Anne Cahill for helpful discussions. This work was supported by a grant of the Deutsche Forschungsgemeinschaft to M.B. and C.B.

REFERENCES

Axelrod, D., N. L. Thompson, and T. P. Burghardt. 1983. Total internal reflection fluorescent microscopy. *J. Microsc.* 129:19–28.

Bastmeyer, M., M. Bähr, and C. A. O. Stuermer. 1993. Fish optic nerve oligodendrocytes support axonal regeneration of fish and mammalian retinal ganglion cells. *Glia.* 8:1–12.

Bastmeyer, M., G. Jeserich, and C. A. O. Stuermer. 1994. Similarities and differences between fish oligodendrocytes and Schwann cells in vitro. *Glia.* 11:300–314.

Braun, D., and P. Fromherz. 1997. Fluorescence interference-contrast microscopy of cell adhesion on oxidized silicon. *Appl. Phys. A.* 65: 341–348.

Burmeister, J. S., G. A. Truskey, and W. M. Reichert. 1994. Quantitative analysis of variable-angle total internal reflection fluorescence microscopy (VA-TIRFM) of cell/substrate contacts. *J. Microsc.* 173:39–51.

Burmeister, J. S., L. A. Olivier, W. M. Reichert, and G. A. Truskey. 1998. Application of total internal reflection fluorescence microscopy to study of cell adhesion to biomaterials. *Biomaterials.* 19:307–325.

Curtis, A. S. G. 1964. The mechanism of adhesion of cells to glass: a study by interference reflection microscopy. *J. Cell Biol.* 20:199–215.

Davies, P. F., A. Robotewskiyi, and M. L. Griem. 1993. Endothelial cell adhesion in real time. *J. Clin. Invest.* 91:2640–2652.

Davies, P. F., A. Robotewskiyi, and M. L. Griem. 1994. Quantitative studies of endothelial cell adhesion. *J. Clin. Invest.* 93:2031–2038.

Driscoll, W., and W. Vaughan. 1978. Handbook of Optics. Optical Society of America, New York.

Izzard, C. S., and L. R. Lochner. 1976. Cell-to-substrate contacts in living fibroblasts: an interference reflexion study with an evaluation of the technique. *J. Cell Sci.* 21:129–159.

Gingell, D. 1981. The interpretation of interference-reflection images of spread cells: significant contributions from thin peripheral cytoplasm. *J. Cell Sci.* 49:237–47:237–247.

Knoll, W. 1991. Optical characterization of organic thin films and interfaces with evanescent waves. *Mat. Res. Soc. Bulletin.* 16:29–39.

Kolega, J., M. S. Shure, W. T. Chen, and N. D. Young. 1982. Rapid cellular translocation is related to close contacts formed between various cultured cells and their substrata. *J. Cell Sci.* 54:23–34.

Lanni, F., A. S. Waggoner, and D. L. Taylor. 1985. Structural organization of interphase 3T3 fibroblasts studied by total internal reflection fluorescence microscopy. *J. Cell Biol.* 100:1091–1102.

Macleod, H. A. 1986. Thin film optical filters. Bristol: Hilger.

Mrksich, M., and G. Whitesides. 1996. Using self-assembled monolayers to understand the interactions of man-made surfaces with proteins and cells. *Annu. Rev. Biophys. Biomol. Struct.* 25:55–78.

Paddock, S. W. 1989. Tandem scanning reflected-light microscopy of cell-substratum adhesions and stress fibres in Swiss 3T3 cells. *J. Cell Sci.* 93:143–146.

Panayotou, G., M. D. Waterfield, and P. End. 1993. Riding the evanescent wave. *Curr. Biol.* 3:913–915.

Rädler, J., and E. Sackmann. 1993. Imaging optical thickness and separation distances of phospholipid vesicles at solid surfaces. *J. Phys. II France.* 3:727–748.

Raether, H. 1988. Surface Plasmons. Springer Verlag, Berlin, Heidelberg, New York.

Rothenhäusler, B., and W. Knoll. 1988. Surface-plasmon microscopy. *Nature.* 332:615–617.

Sambles, J. R., G. W. Bradbery, and F. Yang. 1991. Optical excitation of surface plasmons: an introduction. *Contemp. Phys.* 32:173–183.

Verschueren, H. 1985. Interference reflection microscopy in cell biology: methodology and applications. *J. Cell Sci.* 75:279–301.